Numerical Computations of Advanced Water-Cooled Cold Plates for Thermal Management of Microchips with Hotspots

Matthew Selvaggio, Mahdi Farahikia, Ping-Chuan Wang, Eric Rosenfield, & Alexander Gorzula*

Division of Engineering Programs, State University of New York at New Paltz, New Paltz, NY

https://doi.org/10.33697/ajur.2026.168

Students: selvaggm1@newpaltz.edu, rosenfie1@newpaltz.edu, gorzulaa1@newpaltz.edu
Mentors: farahikm@newpaltz.edu, wangp@newpaltz.edu*

ABSTRACT
Thermal and hydraulic performances of several cold plate designs suitable for 3-D printing are analyzed using finite element analysis (FEA). Computers lie at the center of today's modern world of technology. As technology keeps progressing, greater processing power of these chips is increasingly demanded and this has led to significant challenges, including overheating, uneven microchip temperature distribution, and localized areas of high temperatures known as hotspots, reducing their reliability and lifespan. Conventional cooling techniques, such as air cooling, often fall short of addressing these problems. Liquid-cooling, micro-channel structures known as cold plates, are developed to address such thermal challenges. In this study, five cold plate designs suitable for 3-D printing are analyzed using FEA. The objective of this study is to assess the effects of varying internal geometries and coolant flow rate on thermal and hydraulic performance. The thermal performance was quantified by the thermal resistance and chip temperature uniformity, while the hydraulic performance was quantified by pressure drop and pump power. Results show cold plates with the highest flow rate and more pin-fins near the hotspot than the rest of the cold plate, specifically Model E, outperforms traditional designs in terms of thermal resistance by 3.67%, but at a cost of 120% increase in pump power requirement.

KEYWORDS
Cold Plate; Hotspots; Thermal Management of Microelectronics; Water-Cooled Cold Plates; Computer Chips; Liquid Cooling; Additive Manufacturing Cold Plates; Numerical Analysis of Cold Plates

INTRODUCTION

Today's computers can perform a seemingly infinite number of tasks for industry, transportation, science, or simply personal use. Whether it be a desktop computer or a server room full of computers, one fact remains constant: the demand for higher computing power is increasing. At the core of the high-performing computers and electronics are microchips that run millions of calculations in short periods of time, essentially acting as the brains of these devices. This comes at the cost of the computing units of our electronics experiencing extremely high temperatures and nonuniform temperature distributions[1–4].

Excessive and nonuniform heat negatively impacts the performance and longevity of electronic devices. If a computer becomes too hot, the internal chips could catch fire, which is catastrophic for obvious reasons. The nonuniform distribution of temperature causes warpage and dangerous stresses in the microchips that reduce their lifespan. These and the demand for reliable computers that accommodate nonstop computations warrant the need for effective thermal management of microchips[1–4].

Numerous methods have been introduced to remedy the heat problems at the chip level. Air-cooled heat sinks work on the basis of natural convection heat transfer through fins and pin-fins. Fans were introduced to remove heat from the chips through forced convection heat transfer. However, air-cooled heat sinks fall short of providing proper chip-level heat transfer that meets the demand of high-performing computers, i.e., the chip temperature remains high and is nonuniformly distributed[1, 2, 4].

Combining the better convection coefficient of liquids, such as water, than that of air with the proven advantage of fins in heat transfer, micro-channeled liquid-cooled cold plates were introduced by Tuckerman and Pease in 1981[4]. As coolant flows into these cold plates and their internal micro-channels, it picks up heat. The inlet velocity and temperature of the coolant and whether the flow is laminar or turbulent play important roles in improving heat transfer from the chips. Despite their advantage over air-cooled heat sinks, the traditional cold plates do not lead to a desired quasi-uniform temperature distribution for chips with localized areas of high temperature, known as hotspots. As a result, researchers have been exploring alternatives or alternate cold plate designs that enhance chip-level temperature distribution[4].

Hybrid cold plate designs with pin-fins located on the hotspot and "channel" fins on the background area of the chip are examples of such alternative internal structures. Varying the channel width within the cold plates from a few microns to a few millimeters and the fin height have been examined for thermal and hydraulic performance for both laminar and turbulent flows. In addition to straight channels, some researchers have investigated the efficiency of cold plates with wavy channel profiles[3, 4].

Alongside the internal geometry, the material for the cold plate is an important consideration that affects its overall heat transfer capabilities. While aluminum has traditionally been the most common material of choice, copper has found more application in cold plate manufacturing thanks to its thermal conductivity. Its versatility is further enhanced by its structural integrity, natural antimicrobial properties, corrosion resistance, and cost-effectiveness, making it suitable for a broad range of applications in the thermal management of microelectronics[5].

Despite the theoretical understanding of the advantages of micro-channel cold plates and hybrid designs that enable proper heat transfer from chips with nonuniform power maps due to the presence of hotspots, realizing the various designs that show promising results via computer simulations has been difficult (if not impossible) due to manufacturing challenges. For instance, the fabrication of micro-channels with high precision using conventional methods is virtually impractical. In addition, conventionally manufactured cold plates usually lack a top surface. They have an open top surface that needs to be closed by other means to ensure a safe flow of liquids within the cold plates inside the electronic devices.

Several studies have investigated wavy microchannel cold plate designs through numerical and experimental approaches[8–12]. Numerical analyses by Ghorbani et. al. revealed that increasing the amplitude-to-wavelength ratio of curved channels enhances heat transfer and improves chip-level temperature uniformity[8]. However, Mohammed et al. found that these benefits reach a limit, as further increases in the amplitude-to-wavelength ratio do not sustain performance improvements in aluminum cold plates[9]. Experimental results for sinusoidal wavy microchannel copper cold plates supported these findings, showing similar thermal trends but also indicating a higher pressure drop compared to straight-channel configurations[10].

Variable-wavelength wavy microchannels have also been analyzed numerically under uniform chip heat flux conditions[11]. This design demonstrated improved local thermal performance, particularly for hotspot regions where smaller wavelengths were applied to high-temperature zones. Further simulations indicated that reducing the wavelength or increasing the amplitude of the curves along the flow direction decreases thermal resistance and minimizes on-chip temperature differences in silicon cold plates subjected to uniform heat flux[12].

The advancement of additive manufacturing (AM) provides a promising solution to the manufacturing challenges of sophisticated cold plate designs[4]. Finer channel widths at exceptional precision and the ability to fabricate virtually any internal structure with closed top surfaces are among the advantages of using AM for cold plate manufacturing to remedy the thermal challenges of modern high-performance computers described above. While AM promises these advantages, it comes with its limitations. For example, when printing the ceiling of the cold plate (closed top surface) attention must be given while designing the cold plates in computer-aided design (CAD) programs to ensure they meet these design limitations.

It is evident that numerous modifications of Tuckerman and Pease's microchannel cold plate, as well as combinations of various cooling methods, have been explored. However, differences exist among these studies in how the performances of these cooling methods are compared. These variations include factors such as chip power distribution (uniform or non-uniform), materials used for the cold plate and coolant, performance evaluation metrics, and coolant inlet flow conditions. To the best of our knowledge, a comparative assessment of different internal cold plate designs that accounts for metal 3-D printing constraints and incorporates the manifold has not been extensively investigated.

This paper assesses the impact of various geometries of the internal structures of hybrid cold plates on their thermal and hydraulic performance using finite element analysis (FEA) in COMSOL Multiphysics program. The cold plates are designed in SolidWorks commercial 3-D CAD program while taking into account the limitations of AM. For instance, overhangs are used to prevent the top surfaces of the cold plates from collapsing during 3-D printing. It is known that as the cold plate channels become narrower, the cost of pumping power required for coolant flow increases[4, 6]. The authors aim to achieve an understanding about the performance of each design using computational simulations, 3-D print the cold plates using the CAD models, and to develop a methodology and system for characterization of printed cold plates. The computational simulations provide an insight on how the overhangs and other AM limitations impact the pump power and thermal performance of the cold plates.

Fabricating the complex cold plate designs studied in this work is feasible thanks to the recent advent of metal additive manufacturing (AM) techniques. For instance, Desktop Metal Studio System™ 3-D printers used by Hudson Valley Additive Manufacturing Center (HVAMC) at SUNY New Paltz employ bound metal deposition of 99.9% pure copper. Though the experimental characterization of the cold plates is not the scope of this study, the authors are currently conducting measurements to verify the results obtained from FEA.

METHODS AND PROCEDURES

The methods described below are based on those described in our previous work[4]. The difference and novelty here is that the models are created in a separate CAD program (SolidWorks, specifically) and then imported into COMSOL Multiphysics program. This is because the CAD models are used for 3-D printing for future experimentation to validate the results from the numerical methods explained here. The design practices here take into consideration the limitations of metal 3-D printing as explained above, whereas most (if not all) works described in the literature introduce simplified designs. This makes the results from this work more representative of actual results.

The simulations in this study were conducted using COMSOL Multiphysics, a commercial multiphysics simulation platform. While COMSOL is often categorized as a finite element method based code, its numerical framework is specifically designed to accommodate tightly coupled multiphysics problems. Rather than relying on user-defined element formulations for individual physical phenomena, COMSOL allows governing equations from different physics to be combined at the equation level and solved in a unified framework through its patented modeling approach[16]. This approach enables robust coupling between solid heat conduction and fluid flow without requiring separate solvers or loosely coupled interfaces.

In the present work, a steady-state conjugate heat transfer analysis was performed, in which heat conduction in the solid domains is coupled with laminar fluid flow and convective heat transfer in the fluid domains. The temperature

fields in both the fluid and solid regions are solved simultaneously[13]. Solid-domain heat transfer is discretized using the finite element method, while the fluid flow and convective heat transfer equations are treated using COMSOL's CFD formulation, which employs stabilized finite-element techniques that are mathematically equivalent to finite-volume approaches commonly used in computational fluid dynamics.

The resulting system of equations was solved using a segregated solution strategy. An Algebraic Multigrid (AMG) method was used to efficiently handle the large linear systems, and the Generalized Minimal Residual (GMRES) iterative solver was used for robustness. Convergence was defined as achieving a relative linear residual below 10^{-3}. Lastly, static analysis was used to evaluate the steady-state thermal-fluid response.

CAD Modeling of Cold Plates

Five distinct cold plate geometries were developed using SolidWorks to investigate the influence of geometric variation on thermal and hydraulic performance. Each cold plate incorporates a centrally located pin-fin array occupying a 10×10 mm^2 area, which is assumed to be positioned directly above the primary thermal hotspot of a microelectronic chip with an overall area of 25×25 mm^2. This localized pin-fin region is intended to enhance heat transfer in the area of highest thermal loading.

Figure 1 displays the different key dimensions of each coldplate. The channel, wall, and pin fin sizes vary for each design within a range of 0.5 mm to 1.6 mm. **Figure 2** displays the different models of each cold plate design as an eighth of each geometry and detailed dimensions in the caption. The variable dimensions of each cold plate design are also given in **Table 1**. Despite these variations, all cold plate designs share a common set of baseline dimensions to ensure a consistent comparison. Each model includes a base surface thickness of 3 mm, a top surface thickness of 3 mm, and a cylindrical inlet and outlet with internal diameters of 3 mm, and external diameters of 5 mm. The overall length of each cold plate is 50 mm, with an internal channel height of 6 mm and a total external height of 12 mm. These fixed dimensions are given in **Table 2**, and are visually shown in **Figure 5 A**.

Simulation of Fluid Flow and Conjugate Heat Transfer

The thermal and fluid performances of each cold plate were analyzed using the commercial numerical simulation program COMSOL Multiphysics. This study employed Conjugate Heat Transfer physics, which integrates heat conduction within solid materials, the convective heat transfer within the fluid domain, and the fluid dynamics equations. Copper was chosen as the material for the solid domain, and liquid water was selected for the fluid domain. The density (ρ), specific heat (c_p), thermal conductivity (k), and dynamic viscosity (μ) of liquid water ($273.15\ \text{K} < T < 373.15\ \text{K}$), used

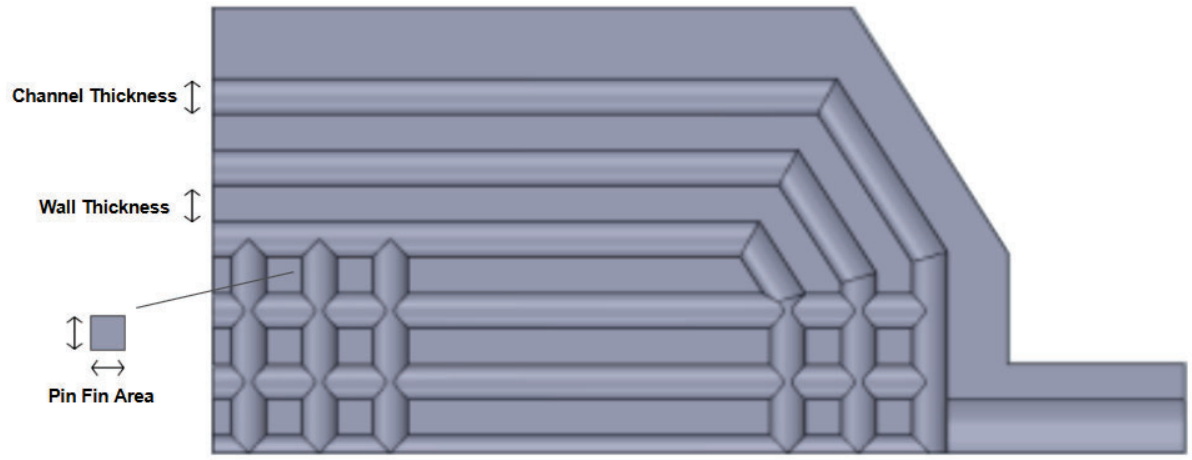

Figure 1. Cold plate Dimension Diagram.

in COMSOL, are as follows:

$$\rho = 0.00006T^3 - 0.06037T^2 + 18.92294T - 950.70406 \quad \textbf{Equation 1.}$$

$$c_p = 12010.1471 - 80.4073T + 0.3099T^2 - (5.3817 \times 10^{-4})T^3 + (3.6254 \times 10^{-7})T^4 \quad \textbf{Equation 2.}$$

$$k = -0.8691 + 0.0089T - (1.5837 \times 10^{-5})T^2 + (7.9754 \times 10^{-9})T^3 \quad \textbf{Equation 3.}$$

$$\mu = 1.3799 - 0.0212T + (1.3605 \times 10^{-4})T^2 - (4.6454 \times 10^{-7})T^3 + (8.9043 \times 10^{-10})T^4 - (9.0791 \times 10^{-13})T^5 + (3.8457 \times 10^{-16})T^6 \quad \textbf{Equation 4.}$$

In these equations, T denotes the temperature in kelvin. The water material model presented in **Equations 1-4** was validated against the correlations provided in the text by Incropera[15], over a range of temperatures expressed in degrees Celsius. As illustrated in **Figure 3**, strong agreement is observed between the two material models across the investigated temperature range. Within the conjugate heat transfer framework, the resulting convective heat transfer behavior is therefore inherently dependent on both space and temperature. Rather than assuming a constant or uniform convection coefficient, COMSOL accounts for local variations in heat transfer through the resolved fluid flow and energy transport coupled with temperature-dependent material properties. Since these default property models were retained and not replaced with constant values, the simulations inherently capture spatial and thermal variations in convective heat transfer without the need to explicitly prescribe the convection coefficient.

Material properties of the copper and TIM used in this study are given in **Table 3**. This approach allowed for a detailed understanding of how heat is absorbed from the chip's surface, transferred through the cold plate, and dissipated by the cooling fluid.

The simulations were conducted under the assumption of laminar flow, a flow regime characterized by smooth, orderly motion of fluid particles along well-defined streamlines, unlike turbulent flow, where fluid motion is chaotic and char-

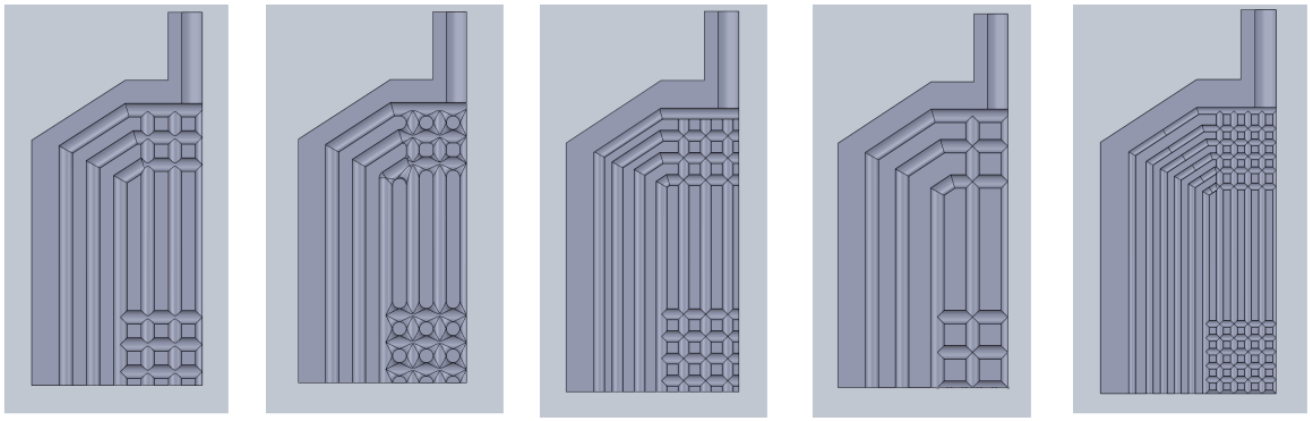

Figure 2. One-eighth models of cold plate. A. Model A: Cold plate with 1.0 mm thick walls, channels, and 1.0 mm thick square pin fins. B. Model B: Cold plate with rounded edges, 1.0 mm thick walls, channels, and 1.0 mm diameter circular pin fins. C. Model C: Cold plate with 0.8 mm thick walls, channels, and 0.8 mm thick square pin fins. D. Model D: Cold plate with 1.6 mm thick walls, 1.0 mm thick channels, and 1.6 mm thick square pin fins. E. Model E: Cold plate with 0.5 mm thick walls, channels, and 0.5 mm thick square pin fins.

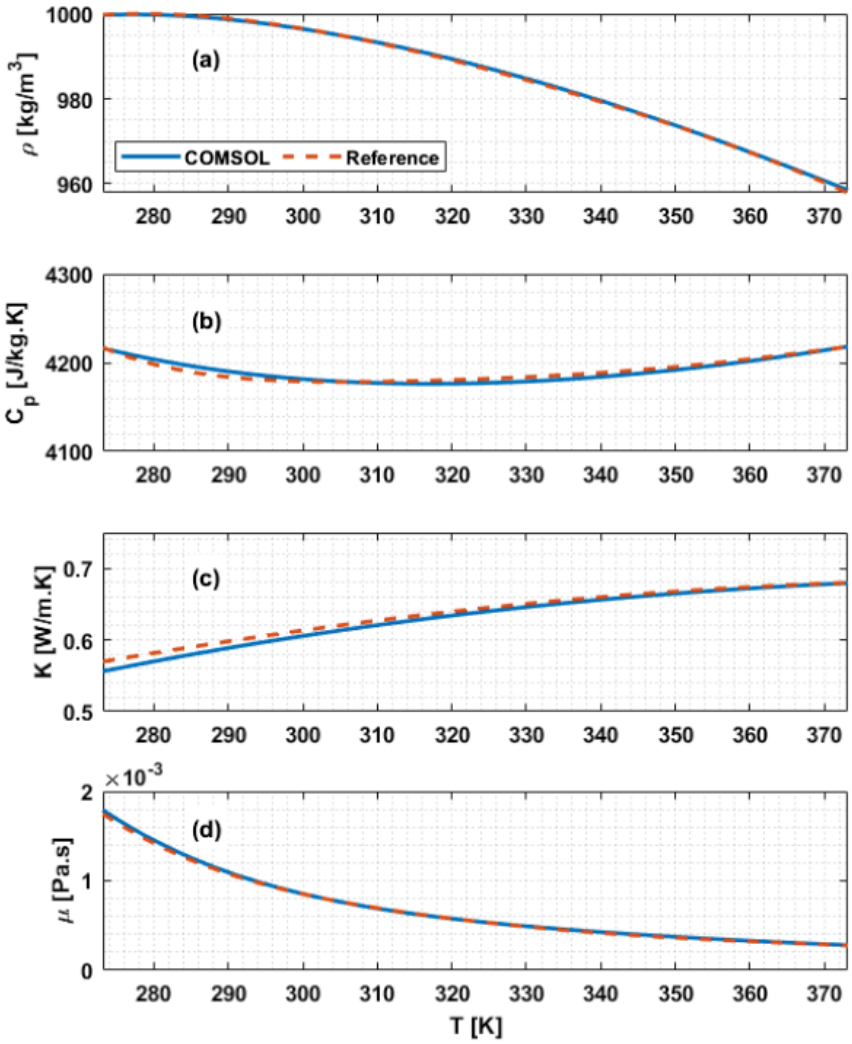

Figure 3. The material model for water, (a) density, (b) specific heat, (c) conductivity, and (d) dynamic viscosity used by COMSOL compared to Reference [15]

Model	Wall Thickness (mm)	Channel Thickness (mm)	Pin fin Dimensions
A	1.0	1.0	1.0×1.0 mm^2 square
B	1.0	1.0	1.0 mm-diameter circle
C	0.8	0.8	0.8×0.8 mm^2 square
D	1.6	1.0	1.6×1.6 mm^2 square
E	0.5	0.5	0.5×0.5 mm^2 square

Table 1. Cold plate design parameters.

acterized by mixing and eddies. Laminar flow is typically described by its low Reynolds number, which depends on factors such as fluid velocity, characteristic length, and viscosity. In the context of this study, the laminar flow regime allowed for precise control of flow rates by setting low inlet fluid velocities and the isolation of thermal transfer phenomena without the added complexities introduced by turbulence. Using this flow assumption, the study focused on understanding the relationship between design parameters and the thermal and hydraulic response of the cold plates.

Figure 4 displays the schematic of the computer chip as used in the simulation. The chip has an area of 25×25 mm^2. The hotspot region is considered a 10×10 mm^2 area at the center of the chip, and the remainder of the chip is con-

Symbol	Definition	Value(mm)
t_W	Top/Base Surface Thickness	3.0
L_{CP}	Cold plate Length	50.0
h_{INT}	Cold Plate Internal Height	6.0
h_{INT}	Overall Cold Plate Height	12.0
d_{INT}	Inlet/Outlet Internal Diameter	3.0
d_{EXT}	Inlet/Outlet External Diameter	5.0

Table 2. Common Dimensions for All Cold plates.

	$c_p(\frac{J}{kg \cdot K})$	$k(\frac{W}{m \cdot K})$	$\rho(\frac{kg}{m^3})$
Copper	385	400	8960
TIM	1200	3	2600

Table 3. Thermophysical properties of copper and TIM.

sidered the background, experiencing lower heat power. The background region was given a heat power of 10 Watts, while the hotspot was given a heat power of 15 Watts. The difference in heat sources between the two regions simulates the hotspot phenomenon, where high heat flux is concentrated at the center region of the chip. This leads to a nonuniform temperature distribution on the chip surface. The connection between the cold plate and the chip is facilitated by a 0.1 mm thin layer of thermal interface material (TIM), modeled as a thermal grease, shown in **Figure 5 A**. The purpose of TIM is to ensure the cold plate sticks to the chip, although its low heat conductivity has a negative impact on the thermal performance of all heat sinks.

This study focused on a parametric analysis, where the inlet velocity of the cooling fluid was varied systematically, starting at 0.05 m/s and increasing incrementally by 0.05 m/s up to 0.3 m/s. The low inlet fluid velocities ensure Reynold numbers that correspond to laminar flows through the cold plates. The laminar flow assumption is validated using the Reynolds number given by

$$Re = \frac{\rho_f u_{avg} D_h}{\mu_f} \qquad \textbf{Equation 5.}$$

in which u_{avg} is the average fluid velocity, and D_h is the hydraulic diameter. For channels with rectangular cross-sections, D_h is given by

$$D_h = \frac{4A_C}{P_C} = \frac{2w_C h_C}{(w_C + h_C)} \qquad \textbf{Equation 6.}$$

where A_C is the mini-channel cross-section area, P_C is the mini-channel cross-section perimeter, and w_C and h_C are the mini-channel width and height, respectively. The Reynolds number in the channels and the inlet with dimensions and the highest coolant inlet velocity mentioned above range between 190 and 2100, which is below the threshold of the turbulent regime (2300). The inlet fluid temperature was set to 293.15 K.

This parametric approach provided several key benefits. It allowed for a comprehensive understanding of how flow rate variations impacted the cold plates' thermal behavior. The cold plates were simulated using a half model and a symmetry analysis along the symmetry plane displayed in **Figure 5 B**. Using the half-symmetry boundary condition helped reduce the computation run-time and required less computational power than a full-model analysis.

In **Figure 5 A**, the coolant enters the cold plate through the inlet velocity surface and exits through the outlet, constant pressure surface. Constant heat fluxes, as defined earlier, are applied to both the hotspot and the background regions. All external surfaces of the cold plate, except for the symmetry plane, are treated as adiabatic. A zero-gradient boundary condition is imposed on the symmetry plane, indicated by the red dashed area shown in **Figure 5 B**. Additionally, all interior walls of the cold plate (except the symmetry plane) are assigned a no-slip boundary condition shown in **Figure 5 C**.

The thermal and hydraulic performance of the designs is evaluated using several parameters found in the literature[4, 7] and described in the following.

Chip Temperature Uniformity

Since one of the main objectives of the advanced cooling methods is to achieve a quasi-uniform temperature gradient on the chip, this is quantified using chip temperature uniformity given by[4]

$$\psi = \frac{T_{c,max} - T_{in}}{T_{c,min} - T_{in}}. \quad \textbf{Equation 7.}$$

Here, $T_{c,max}$ and $T_{c,min}$ represent the maximum and minimum chip temperatures, and T_{in} is the inlet coolant temperature. For a completely chip uniform temperature distribution, it is required that $\psi = 1$.

Thermal Resistance

Another important parameter is the thermal resistance which quantifies the opposition to heat flow through the cold plate. A lower R_{th} indicates that the cold plate can effectively transfer a large amount of heat, which is critical for maintaining the stability and performance of high-powered microchips by cooling down the chip. Thermal resistance is calculated using[4]

$$R_{th} = \frac{A_{CH}(T_{c,max} - T_{in})}{\dot{q}_{CH}} \quad \textbf{Equation 8.}$$

where $T_{c,max}$ is the maximum chip temperature, T_{in} is the inlet coolant temperature, A_{CH} refers to the chip area (here, 25×25 mm^2), and $\dot{q}_{CH}$ refers to the total heat flux experienced by the chip (25 W here).

Chip Maximum and Minimum Temperatures

Chip maximum and minimum temperatures, calculated as given below, determine the effectiveness of chip thermal uniformity based on overcooling or undercooling of the chip. It shows whether an almost "uniform" chip temperature is at safe or dangerous levels.

$$\Delta T_{max} = T_{c,max} - T_{in} \quad \textbf{Equation 9.}$$

$$\Delta T_{min} = T_{c,min} - T_{in} \quad \textbf{Equation 10.}$$

Pump Power Requirements

Pump power is a metric for evaluating the hydraulic performance of the cold plate as it indicates the energy costs of the operation. To increase the speed of flow, it is a factual assumption that more pump power is required to flow the

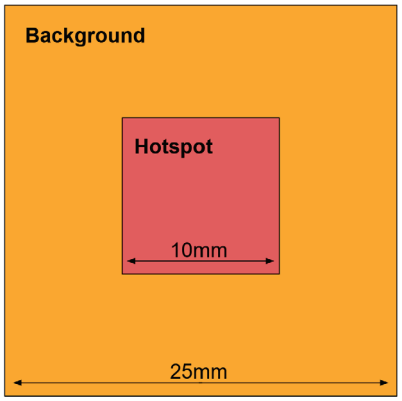

Figure 4. Depiction of square 25×25 mm^2 chip area defined by background and a 10×10 mm^2 hotspot regions.

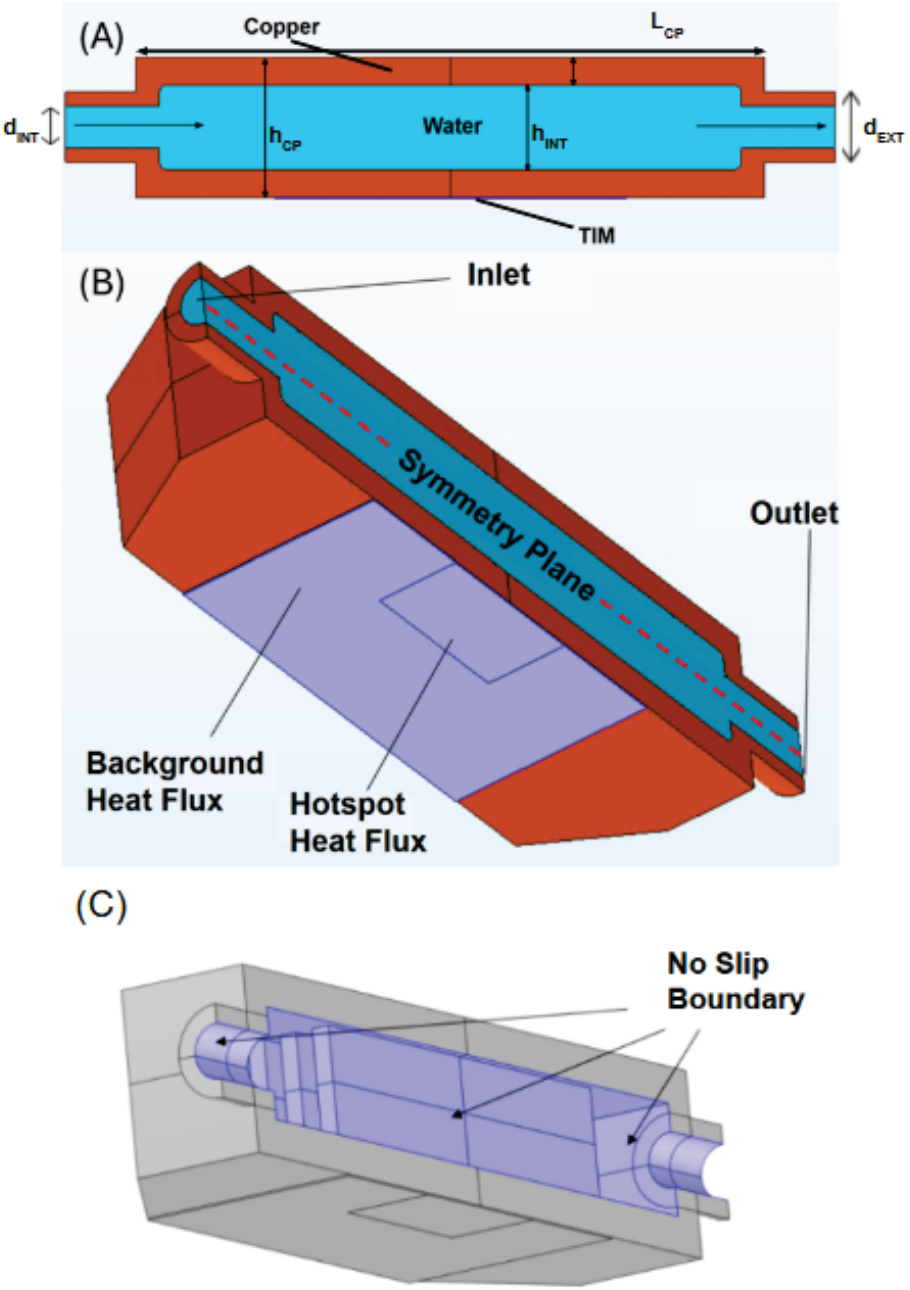

Figure 5. Schematic of cold plate. A. Side view of the cold plate as water flows through with thermal grease depicted along the bottom edge. B. Cold plate boundary conditions. C. Cold plate No-Slip Condition.

coolant into the cold plate. Quantifying the pump power is necessary for understanding the cost of operation on a more accurate level. The calculation of pump power requires the pressure drop (Δp), the inlet coolant velocity (v_{in}), and the cross-section area of the inlet port A_{in} and is given by **Equation 11**[4]. The cross-section of the inlet port is a circle, so the area is equal to πr_{in}^2. The cross-sectional area would then be equal to 0.000625 m^2.

$$P = \Delta p(v_{in}A_{in}) \qquad \textbf{Equation 11.}$$

Mesh Type	Number of Elements	Thermal Resistance (K/W)	Relative Change
Extra Coarse	28659	15.733	NA
Very Coarse	192229	12.258	28.343%
Coarse	494556	10.376	18.137%
Normal	1803042	7.889	31.527%
Fine	6572749	7.728	2.090%
Finer	12764457	7.598	1.308%

Table 4. Element Count and Thermal Resistance for each Mesh.

RESULTS

Mesh-Dependence Analysis

A mesh refinement study conducted on Model E to evaluate numerical convergence of the thermal resistance prediction which is shown in **Table 4**. Six systematically refined meshes were analyzed, ranging from an extra coarse mesh with 28,659 elements to a finer mesh with 12,764,457 elements. Thermal resistance was selected as the primary global quantity of interest, as it directly reflects the overall heat transfer performance of the system. Relative changes in thermal resistance were computed between successive mesh levels to assess convergence behavior. As the mesh was refined, the predicted thermal resistance decreased and approached an asymptotic value. This convergence behavior is evident in the plateau region highlighted by the red box in **Figure 6**, which corresponds to the Normal mesh containing approximately 1.8 million elements. The relative change in thermal resistance between the normal and fine meshes was 2.090%, indicating that the solution had largely stabilized at this resolution and further refinement is unnecessary. Based on this trend, the Normal mesh was selected for the remainder of the study as a balance between numerical accuracy and computation time.

Thermal and Hydraulic Analysis

The post-processing of the simulations involved an extensive temperature analysis of the cold plate to determine its heat transfer characteristics. The key characteristics included chip temperature uniformity (ψ), maximum and minimum temperature differences (T_{max} and T_{min}) between the temperature at the inlet and the chip after cooling, thermal resistance (R_{th}) of the cold plate, pump power (P), and the overall influence of the flow rate on these parameters.

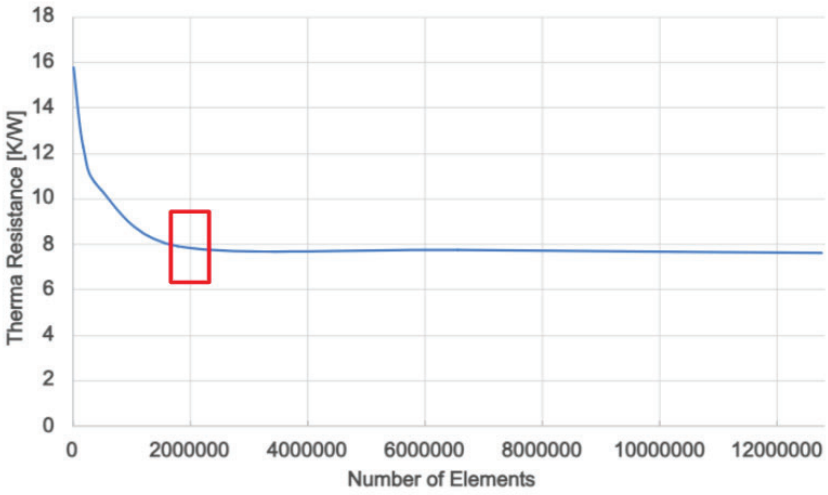

Figure 6. Mesh-dependence analysis - The rectangle shows the chosen element size in this study.

Chip Temperature Uniformity

The temperature gradients of each model are presented in **Figure 7**, which qualitatively illustrates the distribution of chip temperature. In these graphs, the coolant flow is vertical from bottom (closer to the inlet) to top (closer to the outlet). The temperature of the hotspot is observed to be higher than that of the background area of the chip. The highest temperature of the hotspot is at a point closer to the outlet. This is reasonable because water temperature is higher at this point, reducing the heat transfer rate.

Quantitative analyses of the performance of the cold plate models are presented in the following to better understand their thermal and hydraulic efficiency. The chip temperature uniformity results from **Equation 7** are shown in **Figure 8**. It is observed that the chip temperature uniformity is smaller at lower coolant flow rates. As the flow rate increases, the chip temperature distribution becomes more nonuniform. In addition, the chip temperature uniformity shows a bigger gap among the various models studied in this work at higher coolant flow rates.

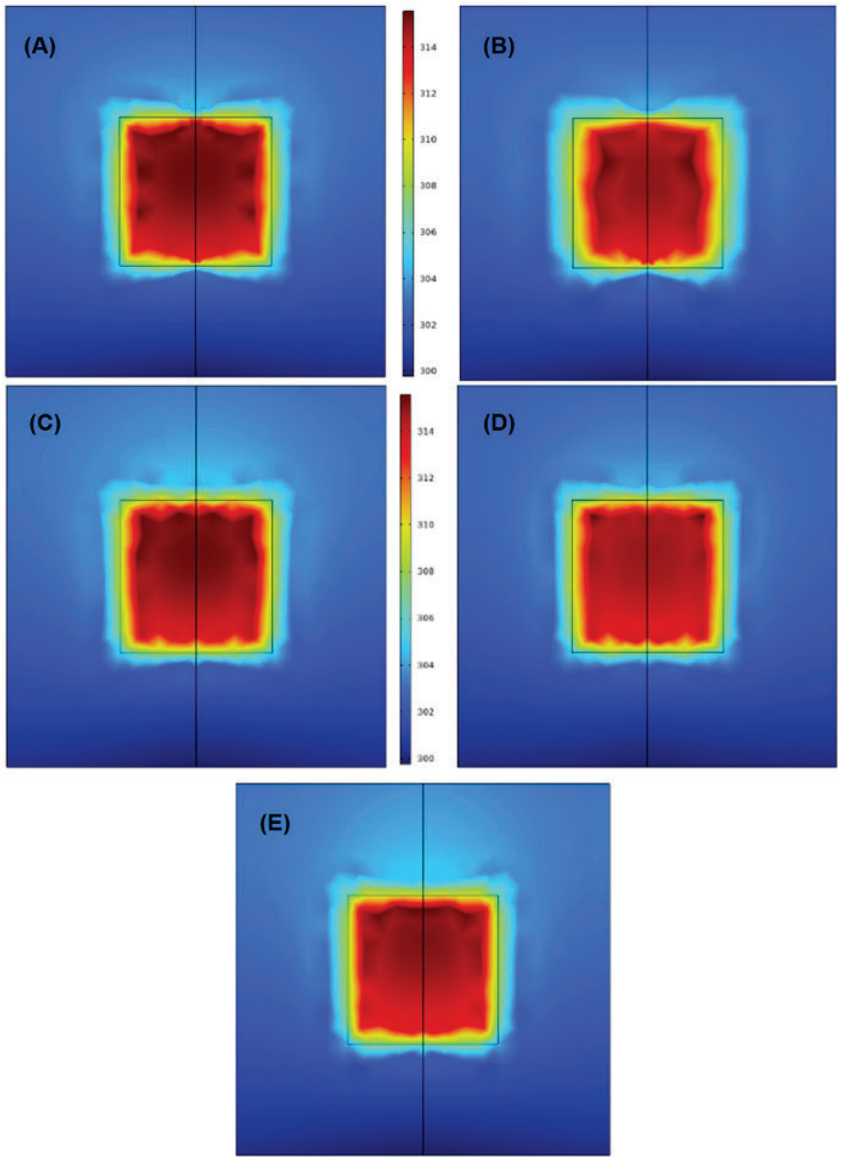

Figure 7. Temperature gradient of computer chip after cooling in Kelvins. A. Model A. B. Model B. C. Model C. D. Model D. E. Model E.

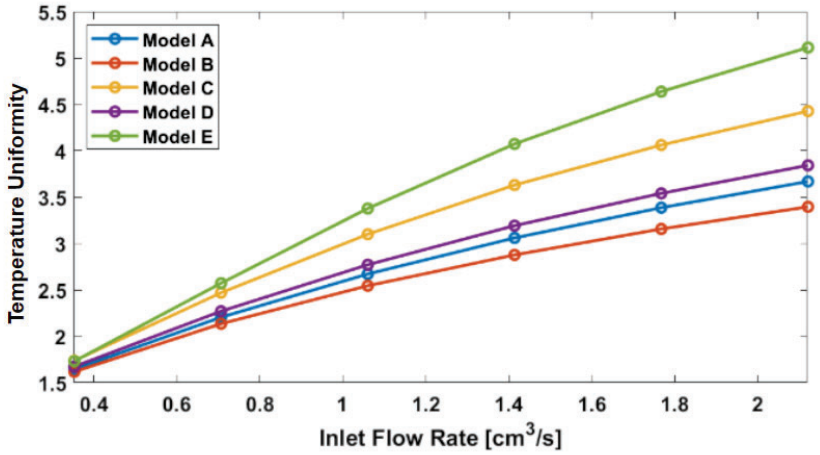

Figure 8. Temperature uniformity as a function of coolant inlet flow rate.

Thermal Resistance

Figure 9 shows the variation of thermal resistance as a function of inlet coolant velocity for all the cold plate designs calculated using **Equation 8** . As the inlet coolant velocity increases, it leads to a greater capacity to absorb and carry away heat from the heated surfaces of the chip. This increased efficiency results in a smaller T_{max} for the same amount of heat transfer, thereby lowering the value of R_{th}. In contrast, lower inlet coolant velocity leads to higher thermal resistance. This is because at lower flow rates, the coolant moves more slowly, allowing more time for heat to build up in the fluid, reducing its heat transfer efficiency. This trend is observed for all the cold plate designs.

Chip Maximum and Minimum Temperatures

The observations from the chip temperature uniformity and thermal resistance of the cold plate lead to a peculiar behavior. Cold plates with lower thermal resistance (i.e., efficient heat transfer) lead to a more nonuniform chip temperature distribution. This is detrimental to the performance and reliability of the chip, as the large temperature gradient across its surface leads to warpages and thermally-induced stress, which eventually cause fracture in solder joints. To understand this contradictory behavior, the maximum and minimum chip temperatures (T_{max} and T_{min}, respectively) for each cold plate design, given below[4], are studied.

Figure 10 conveys the maximum and minimum chip temperature with respect to the inlet coolant flow rate from **Equation 9** and **Equation 10**. While model B shows the smallest chip temperature gradient, its high thermal resistance leads

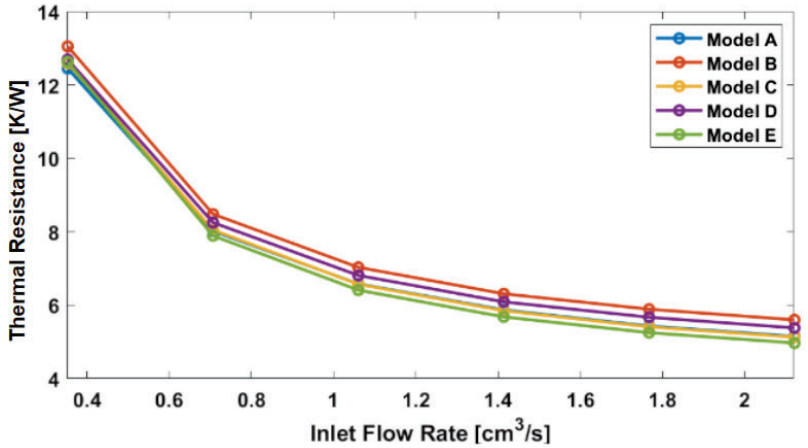

Figure 9. Thermal resistance for each cold plate vs. flow rate.

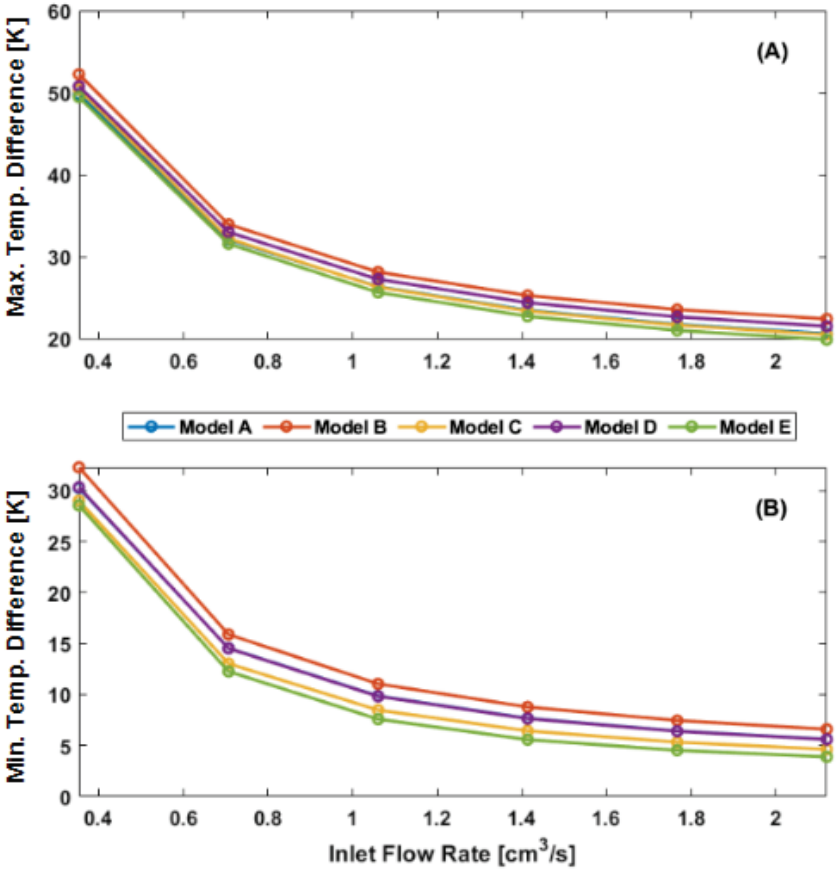

Figure 10. Temperature difference for each cold plate vs. flow rate. (A) Maximum temperature difference (B) Minimum temperature difference.

to higher maximum and minimum temperatures on the chip surface. The difference between these temperatures is low enough to suggest a better temperature uniformity, although the chip may remain dangerously hot. In contrast, model E, that gives the largest non-uniformity in chip temperature distribution, has a lower thermal resistance which leads to lower maximum and minimum chip temperatures. This means model E is more efficient in cooling down the chip on both the hotspot and the background regions. The wider gap between the maximum and minimum chip temperatures achieved by model E results in a higher non-uniformity, while the chip temperature is below that of model B.

While a lower value of ψ means smaller temperature gradient on the chip surface, it is not an indication of the chip temperature. For example, a "good" temperature uniformity may be achieved while the chip temperature is still dangerously high. This can happen if the cold plate design does not provide an efficient heat transfer from the chip. The lower thermal resistance of model E means it has a more efficient heat transfer on both hotspot and background. In other words, the background region of the chip is "over-cooled" with this design. Other methods, such as coolant flow rate control using two inlet ports, can be applied to remedy this.

Pump Power Requirements

Figure 11 shows the pump power with respect to inlet coolant flow rate for all the cold plate designs calculated using **Equation 11**. While higher flow rates improve heat transfer by enhancing convective heat transfer efficiency, they come with the significant drawback of increased pump power requirements. In **Figure 11**, it is shown that the pump power nonlinearly increases as the flow rate increases. Model E, with the reasonably more efficient thermal performance compared to the other designs, also requires more pump power. This is more obvious at higher coolant flow rates. This indicates that achieving a low thermal resistance comes at a higher hydraulic cost.

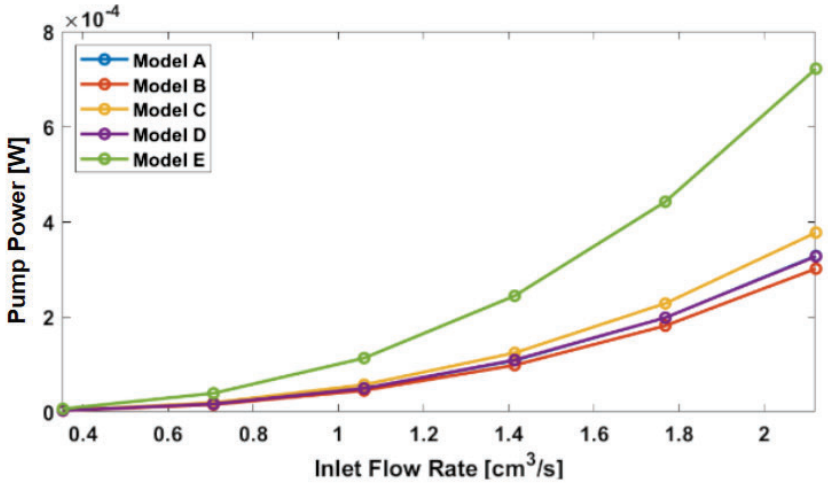

Figure 11. Pump power for each cold plate vs. flow rate.

As the coolant flow rate rises, the resistance to fluid movement within the cold plate's channels also increases due to, for instance, frictional forces. This resistance creates a higher pressure drop within the system needed to sustain the flow rate within the cold plate, which is why overcoming this resistance demands more energy from the pump, leading to higher operational costs and energy consumption. The high pressure drop as a result of the flow rate directly results in the substantial increase in pump power. This trade-off between thermal performance and energy expenditure is a critical consideration in the design of practical thermal management systems.

DISCUSSION

The performance of Model E at 2.1206 cm^3/s flow rate from the current study is compared to those reported in our other work[4] with inlet flow rate of 2.84 cm^3/s, as it has the closest inlet conditions to this work. However, it is important to note that the designs here more closely correspond to the cold plates fabricated using metal 3-D printing, while those in the literature are simplified, and their results do not correspond the effects of design considerations imposed by metal 3-D printing limitations. As such, the better-performing Model E in this work requires slightly higher pump power (0.772 kW) compared to the best-performing design in the reference (0.501 kW)[4].

The temperature uniformity of Model E in the current work at slightly over 5.0 seems considerably higher than the reference at 3.42. However, the temperature levels reached by Model E are lower than the reference, due to more surface area for heat transfer in Model E. As a result, although Model E leads to more temperature non-uniformity at the chip level compared to the literature, it reaches safe operating temperatures. Further modifications of the results in this work may improve their performance. In the following, the performance of Model E is compared with those of the other designs studied in this work.

As mentioned above, Model E exhibited the best performance in terms of heat transfer efficiency among the designs tested. Its superior thermal performance can be attributed to its high-density channel and pin-fin configuration, which maximized the surface area available for convective heat transfer through the coolant. By providing more pathways for the coolant to absorb and dissipate heat, Model E effectively achieved lower thermal resistance R_{th} compared to the other designs. This led to lower overall chip temperatures, also suggesting more nonuniform temperature distribution. Several potential options such as two inlet ports (one with higher coolant flow rate for the hotspot and the other with a lower coolant flow rate for the background) can be applied to remedy this. However, this enhanced heat transfer came at a significant cost: the dense channel arrangement and narrow flow paths created a high resistance to fluid flow, requiring considerably more pump power to maintain the desired flow rates. As a result, while Model E excelled thermally, its high energy demands made it less cost-effective for practical applications.

The study also highlighted the impact of pin geometry on heat transfer performance. Designs with larger pin fins were found to be less efficient in transferring heat compared to those with smaller pins. This is because larger pin dimensions, like that of Model D, reduce the total number of pins that can fit within a given area, effectively decreasing the overall surface area available for heat exchange. Smaller pins, on the contrary, allow for a greater density of fins, creating more interfaces between the coolant and the heated surfaces, thereby enhancing convective heat transfer. This finding highlights the importance of optimizing pin dimensions to balance thermal performance and structural feasibility.

Additionally, square pin fins were shown to outperform round pin fins in terms of heat transfer efficiency. Square pins provide a larger contact surface area than round pins of equivalent thickness in Model B, allowing for greater heat exchange between the cold plate and the cooling fluid. The angular geometry of square pins may promote localized turbulence around the edges as coolant flow rate increases, which can enhance the convective heat transfer process. Turbulent flow is more effective in enhancing the heat transfer rate between materials, and authors plan on studying the effectiveness of such flow regimes with similar cold plate designs. Indentations, ribbing, fins, etc. along the surfaces the water flowed through cause disruptions in the flow pattern. This disruption in flow pattern fosters more mixing of the fluids which, consequently, enhances heat transfer. This makes square pins particularly advantageous in applications where maximizing cooling efficiency is critical.

Finally, the number of channels in the cold plate design had a direct correlation with its thermal performance. Increasing the number of channels increased the surface area available for convective heat transfer, resulting in a higher overall heat dissipation rate. However, this improvement in heat transfer came with potential trade-offs, including higher pressure drops that resulted in increased pump power requirements. Designs with denser channels, such as Model E, demonstrated the benefits of maximizing surface area but also highlighted the challenges of balancing heat transfer efficiency with energy consumption and operational costs.

In summary, the study revealed that while designs like Model E achieved exceptional heat transfer performance through high channel density, their practical utility is limited by the associated energy costs. The findings also emphasized the importance of optimizing pin and channel geometries, with smaller and square pins, as well as increased channel density, providing the best opportunities for enhancing heat transfer without excessively compromising cost-effectiveness. These insights are critical for designing advanced cooling solutions tailored to the needs of high-performance microchips.

Feasibility Demonstration of Experimental Measurement

As mentioned previously, additive manufacturing (AM) enables fabrication of cold plate designs with complex internal configurations that are not feasible with conventional manufacturing techniques. However, certain limitations of this method must be taken into consideration in the design process[14]. For example, the limit of the aspect ratio (i.e., height-to-thickness ratio) of the pin fins and channel walls needs to be determined to ensure the manufacturability and integrity of various enclosed structures. Also, the overhang angle of the pin fins and channel walls needs to be studied to properly self-support the top cover without additional internal support for fabrication.

Although the fabrication and experimental characterization of the cold plate designs assessed in this study is currently in progress, two self-supported cold plate designs with standard straight-channel configurations were fabricated with AM for measurements. **Figure 12 (a) and (b)** illustrate the two six-fin, five-channel designs with 0.8 mm and 1.6 mm

Figure 12. Cold plate designs used for feasibility demonstration of the AM fabrication and experimental characterization capabilities: (a) Model 1: five straight channels with 0.8 mm fin width, and (b) Model 2: five straight channels with 1.6 mm fin width.

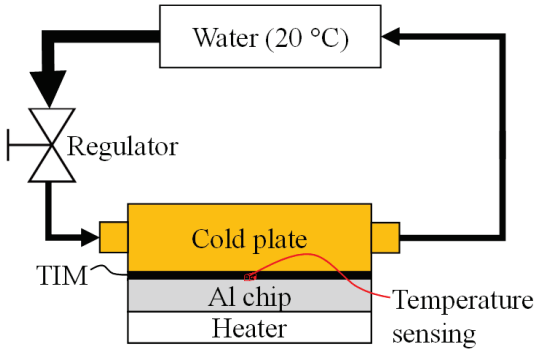

Figure 13. Preliminary experimental setup to demonstrate cold plate efficiency characterization.

fin width, respectively. **Figure 13** shows the schematics of the test setup, where a 25×25 mm^2 aluminum (Al) "chip" with 3.2 mm in thickness was evenly heated with a 30×30 mm^2 metal ceramic heater below. A cold plate was mounted on the Al chip through a thermal interface material (TIM) layer for thermal coupling. Temperature at the center of the Al chip was monitored in real time by a thermocouple inserted between the Al chip and the cold plate. The steady-state temperatures at various heater powers and water flow rates were measured for each cold plate.

Figure 14 (a) shows the characterization of thermal resistance of Model 1, determined from the slope of the steady-state temperature rise versus heater power for each of the six applied flow rates. The experimental uncertainties were within 5% for flow rate and 1% for temperature, as estimated from three repeated measurements at a given condition. **Figure 14 (b)** shows the extracted thermal resistance as a function of flow rate, comparing between the two cold plate models. The trends were fitted with an expected power-law function with reasonable agreement, from which the thermal resistance of Model 2 at a flow rate of 10 g/s was estimated to be about 16% lower than Model 1. A complementary FEA study similar to the process described in this paper was also conducted, where the thermal resistance of Model 2 is about 28% lower than Model 1 at a flow rate of 10 g/s. The qualitative agreement between the experimental and simulation results further supports the soundness of the test methodology, which will be employed to provide empirical data to validate and calibrate the FEA results in this study.

CONCLUSIONS

In conclusion, this study highlights the critical role of cold plate design in managing the thermal challenges of high-performance microchips. It is important to note that the cold plates in this study were designed with the limitations of metal 3-D printing in mind (such as overhangs needed to print the cold plate ceiling) because the authors aim to com-

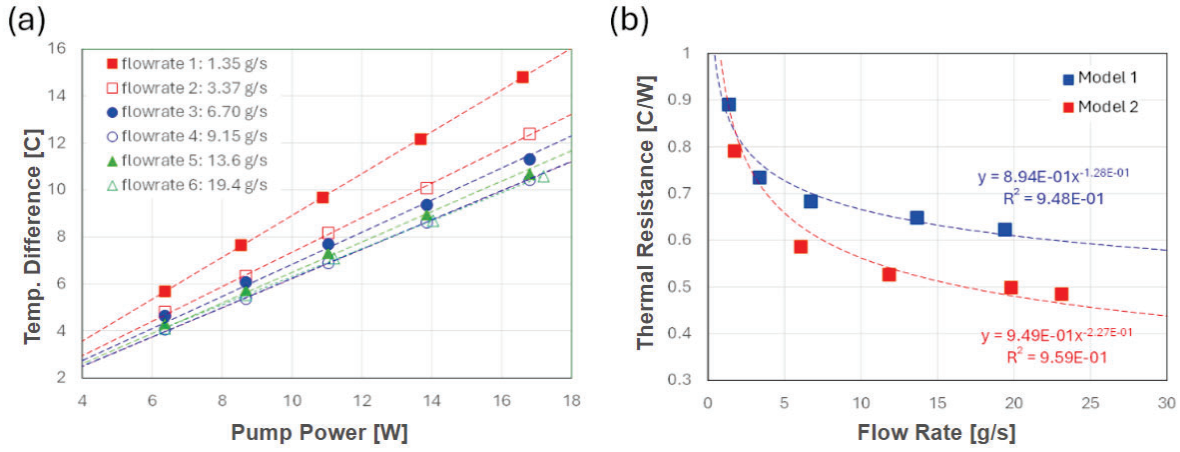

Figure 14. (a) Measured steady-state temperature rise (DT) versus heater power for cold plate Model 1 to determine its thermal resistance at various flow rates, and (2) the extracted thermal resistance as a function of flow rate, comparing between the two cold plate designs.

pare the findings of the present study with measurements. The 3-D models will be used directly for cold plate fabrications using additive manufacturing.

By analyzing the effects of pin geometry, channel density, and coolant flow rate, this research revealed important trade-offs between thermal efficiency and energy consumption. Model E demonstrated exceptional heat transfer capabilities due to its high surface area and dense channel configuration, though its increased pump power requirements limit its cost-effectiveness. Optimized designs with square pins, high channel density, and moderate flow rates provided a balance between performance and operational costs, making them more suitable for practical applications. These findings offer valuable insights for the development of advanced thermal management solutions.

ACKNOWLEDGEMENTS

The authors thank the support and resources of The State University of New Paltz, the Office of Research, Scholarship, and Creative Activities (RSCA), and the Hudson Valley Additive Manufacturing Center (HVAMC).

REFERENCES

1. Philips, Richard J. (1987) Thermal Management of Microelectronics, in *Forced-convection, liquid-cooled, microchannel heat sinks* (Massachusetts Institute of Technology) 27–45. *http://hdl.handle.net/1721.1/14921*
2. Ali, Amir F., El-Genk, Mohamed S. (2012) Spreaders for immersion nucleate boiling cooling of a computer chip with a central hot, *Energy Convention and Management* 53.1, 259–267. *https://doi.org/10.1016/j.enconman.2011.09.007*
3. Xue, Z., Yan, Y., Shen, K., He, Z., You, J. (2024) Thermal performance enhancement of a micro-jet heat sink via parametric investigated micro pin fin arrays, *International Journal of Thermal Sciences* 196, 108717. *https://doi.org/10.1016/j.ijthermalsci.2023.108717*
4. Farahikia, M., Wang, P., Reyes, L., Krumholtz, M. (2024) A Comparative Numerical Analysis of Cold Plates for Thermal Management of Chips With Hotspots, *Journal of Electronics Packaging* 143(3), 034501–034507. *https://doi.org/10.1115/1.4064523*
5. Singh, G., Missiaen, J. M., Bouvard, D., Chaix, J. M. (2021) Copper extrusion 3D printing using metal injection moulding feedstock: Analysis of process parameters for green density and surface roughness optimization, *Additive Manufacturing* 38, 101778. *https://doi.org/10.1016/j.addma.2020.101778*
6. Patil, P. M., Yadav, A. P., Patil, A. P. (2015) Comparative study between heat transfer through laminar flow and turbulent flow, *Int. J. Innoiv. Res. Sci. Eng. Technol.* 4, 2223–2226. *https://api.semanticscholar.org/CorpusID:212552401*
7. Hadad, Y., Radmard, V., Rangarajan, S., Farahikia, M., Refai-Ahmed, G., Chiarot, P. R., Sammakia, B. (2021) Minimizing the effects of on-chip hotspots using multi-objective optimization of flow distribution in water-cooled parallel microchannel heatsinks, *Journal of Electronic Packaging* 143(2), 021007. *https://doi.org/10.1115/1.4048590*
8. Ghorbani, Nima and Targhi, Mohammad Zabetian and Heyhat, Mohammad Mahdi and Alihosseini, Yousef (2022) Investigation of wavy microchannel ability on electronic devices cooling with the case study of choosing the most efficient microchannel pattern, in *Scientific Reports* (Nature Publishing Group UK London) 5882. *https://doi.org/10.1038/s41598-022-09859-6*
9. Mohammed, HA and Gunnasegaran, Prem and Shuaib, NH (2011) Numerical simulation of heat transfer enhancement in wavy microchannel heat sink, in *International Communications in Heat and Mass Transfer* (Elsevier) 63–68. *https://doi.org/10.1016/j.icheatmasstransfer.2010.09.012*
10. Sui, Y and Lee, PS and Teo, CJ (2011) An experimental study of flow friction and heat transfer in wavy microchannels with rectangular cross section, in *International Communications in Heat and Mass Transfer* (Elsevier) 2473–2482. *https://doi.org/10.1016/j.ijthermalsci.2011.06.017*
11. Sui, Y and Teo, CJ and Lee, Poh Seng and Chew, YT and Shu, C (2010) Fluid flow and heat transfer in wavy microchannels, in *International Communications in Heat and Mass Transfer* (Elsevier) 2760–2772. *https://doi.org/10.1016/j.ijheatmasstransfer.2010.02.022*

12. Lin, Lin and Zhao, Jun and Lu, Gui and Wang, Xiao-Dong and Yan, Wei-Mon, C (2017) Heat transfer enhancement in microchannel heat sink by wavy channel with changing wavelength/amplitude, in *International Journal of Thermal Sciences* (Elsevier) 423–434. *https://doi.org/10.1016/j.ijthermalsci.2017.05.013*

13. Xie, XL and Tao, WQ and He, YL (2007) Numerical study of turbulent heat transfer and pressure drop characteristics in a water-cooled minichannel heat sink, in *American Society of Mechanical Engineers Digital Collection* (ASME) 247–255. *https://doi.org/10.1115/1.2753887*

14. Studio System, (2022), Design Guide, February 2022, URL: *https://www.scribd.com/document/853014872/Studio-System-BMD-Design-Guide* (accessed October 2025)

15. Incropera, F. P., DeWitt, D. P., Bergman, T. L., Lavine, A. S., (1996), *Fundamentals of Heat and Mass Transfer*, Vol. 6, Wiley, New York

16. COMSOL, (2020), *Multiphysics versus FEA*, COMSOL Blog, COMSOL AB, URL: *https://www.comsol.com/blogs/multiphysics-versus-fea*

ABOUT THE STUDENT AUTHOR

Matthew Selvaggio is a senior at The State University of New York (SUNY) at New Paltz, pursuing a Bachelor's of the Science of mechanical engineering. Working under the advice of Dr. Mahdi Farahikia and Dr. Ping-Chuan Wang, he is in the process of performing a comparative analysis study between simulation and experimentation of hotspot-based cold plate research surrounding turbulent flow. He plans to attend graduate school following graduation from SUNY new Paltz in December 2025.

PRESS SUMMARY

As demand for high-performance computing in technology and industries increases, managing the high temperatures of the chips (e.g., CPUs and GPUs) that act as the brains of these electronics has become challenging. Data centers, computers that run spaceships, aircraft, cars, and gaming computers are examples of such situations. Due to the high computing demands, the temperatures of the chips rise to dangerously high levels and create nonuniform temperature distributions and localized areas of high heat known as hotspots. These thermal issues negatively impact the reliability and life-span of the electronic devices.

Traditional heat sinks that work based on the convective heat transfer of air do not provide sufficient cooling to mitigate these challenges. As a result, other methods, such as liquid-cooled cold plates, are introduced. These methods take advantage of the better convective heat transfer of liquid coolants, like water, relative to air.

Eliminating the thermal challenges of high-performance computing necessitates advanced cold plate designs that are not easily feasible using traditional fabrication methods. Thanks to additive manufacturing (AM), new designs that can promise enhanced thermal management of microelectronics are achievable. However, there are still limitations in AM that must be considered when designing cold plates.

Numerical methods such as finite element analysis (FEA) provide estimates of the performance of cold plates in the computational world before they are realized through manufacturing. This saves the costs of fabricating and testing prototypes.

This research investigates the impact of various cold plate designs, with consideration of AM limits, on their thermal and hydraulic performance using the commercial Multiphysics program COMSOL. Since cold plates require liquid coolant for heat removal from the chip, the pump power needed for the coolant flow is a factor to be considered in choosing a design. Ultimately, this decision is a trade-off between thermal efficiency and hydraulic cost of the cold plate.